Structure Dependence of Kinetic and Thermodynamic Parameters in Singlet Fission Processes

Structure-Dependence of Kinetic and Thermodynamic Parameters in Singlet Fission Processes.

Daphné Lubert-Perquel[1†*], Anna Szumska[2], Mohammed Azzouzi[2], Enrico Salvadori[3*], Stefan Ruloff[4], Christopher M. W. Kay[4,5], Jenny Nelson[2] and Sandrine Heutz[1*]

[1] London Centre for Nanotechnology and Department of Materials, Imperial College London, Prince Consort Road, London SW7 2BP, U.K.

[2] Department of Physics, Imperial College London, Prince Consort Road, London SW7 2BP, U.K.

[3] Department of Chemistry, University of Turin, Via Giuria 7, Turin 10125, Italy

[4] Department of Chemistry, University of Saarland, 66123 Saarbrücken, Germany

[5] London Centre for Nanotechnology, University College London, 17-19 Gordon Street, London WC1H 0AH, UK.

ABSTRACT: Singlet fission – whereby one absorbed photon generates two coupled triplet excitons – is a key process for increasing the efficiency of optoelectronic devices by overcoming the Shockley-Queisser limit. A crucial parameter is the rate of dissociation of the coupled triplets, as this limits the number of free triplets subsequently available for harvesting and ultimately the overall efficiency of the device. Here, we present an analysis of the thermodynamic and kinetic parameters for this process in parallel and herringbone dimers in co-evaporated films of pentacene in *p*-terphenyl. It was found the rate of dissociation is faster for parallel dimers than their herringbone counterparts, as is the recombination to ground state. DFT calculations, which provide the magnitude of the electronic coupling as well as the distribution of molecular orbitals for each geometry, suggest that decreased triplet coupling in the parallel dimer is the driving force for faster dissociation. Conversely, localization of the molecular orbitals and higher triplet interaction result in slower dissociation and recombination The identification and understanding of how intermolecular geometry promote efficient triplet dissociation provides the basis for control of triplet coupling and thereby the optimization of device performance.

INTRODUCTION

Distance and relative orientation between chromophores dictate the nature and strength of their electronic coupling influencing their behaviour and usefulness in technological applications. Photosynthetic complexes, where the protein scaffold holds chlorophyll and carotenoid chromophores in precisely defined positions, provide striking examples of this. For instance, the precise arrangement of bacteriochlorophylls in the LH2 complex considerably redshifts the absorption wavelength of the complex compared to the monomer.[1,2]

In common organic photovoltaics, where photosynthetic light conversion reactions are mimicked, the active components are distributed within amorphous or polycrystalline structures and the overall efficiency is a weighted average over all possible distances and orientations. Singlet fission (SF) - a mechanism by which one singlet exciton splits into two triplet excitons - has gained prominence as a viable pathway for exceeding the Shockley-Queisser limit – the theoretical maximum efficiency due to non-radiative recombination processes. SF could also improve the efficiency of hybrid organic-inorganic photovoltaic cells, whereby the organic layer harvests high-energy photons and supplies two lower energy photons to the underlying inorganic layer, typically amorphous silicon, where charge separation is accomplished.[3–6] It can be described by the equation:

$$S_0 \rightarrow S_1 \rightarrow {}^1(TT) \rightarrow {}^5(TT) \rightarrow T + T$$

where S_0 and S_1 are the ground and (first) excited singlet states, respectively; $^1(TT)$ are the coupled triplets with singlet multiplicity produced by SF; and T + T are the free triplets available after fission for harvesting. An intermediate step, often labelled $^1(T\ldots T)$ but not shown here, represents the correlated triplet pairs spatially separated whilst retaining spin coherence; a state enabling spin mixing due to weaker coupling that results in quintets[7]. Here we directly use the notation $^5(TT)$ to denote quintets , as they are unambiguously identified using electron paramagnetic resonance (EPR) spectroscopy.[8–10]

Not many organic semiconductors are known to undergo SF mostly because of the strict energetic requirement $E_S \approx 2\,E_T$.[11] Linear acenes and their derivatives are by far the most studied organic semiconductors for SF and there appears to be a correlation between number of benzene units and singlet-triplet energy gap. For instance, SF is endergonic for tetracene and exergonic for pentacene.[12–14] However, although both molecules adopt a herringbone motif in their crystal packing, the

effect of the relative orientation between neighbouring chromophores on the thermodynamics of SF and subsequent exciton migrations has not been investigated.

Several models have been designed to investigate the SF kinetics [15–17], and many attempts at experimentally resolving the kinetic parameters have been reported.[9,10,13,18,19] Nonetheless, several matters remain under discussion, such as the extent of triplet correlation after SF.[7] The exciton delocalisation on non-covalent dimers has been studied,[20–24] although a direct comparison between various molecular configurations and its effect on SF dynamics is lacking. Recent studies have investigated the effect of diffusion on the kinetics revealing that it plays a significant role in the successful dissociation of excitons into free triplets.[25,26]

Calculations have predicted that the slip-stacked geometry is optimal for SF as this configuration results in a substantial orbital overlap.[12,21,24] More recently, a comprehensive modelling of ethylene pairs showed that the slip-stacked arrangement is one of the most efficient pairs for SF.[27] Consequently, covalent dimers of perylene-3,4,9,10-bis(dicarboximide) (PDI) and terrylene-3,4,11,12-bis(dicarboximide) (TDI) with slip-stacked geometries have been synthesised and identified as efficient SF materials in solution.[28–30] In solid-state materials, it has been suggested that both slip-stacked or herringbone structures are suitable, as observed in pentacene and tetracene systems,[31] though a comparison has not been explicitly reported. Furthermore, recent work suggested that the dimer configuration affects the efficiency of quintet dissociation and therefore the potential for triplet harvesting within these layers.[10] Specifically, the ^{5}(TT) state from parallel and herringbone dimers have distinct Hamiltonian parameters and the coupled triplets originating from parallel dimers dissociate more readily.

Here we explore the effect of orientation on the energy landscape of a well-defined pentacene system.[32] We investigate the dissociation kinetics in a dilute systems where diffusion is likely suppressed or can be understood as a function of the pentacene content. The kinetic parameters are obtained as a function of temperature and concentration to identify variations in the dynamics of the parallel, specifically slip-stacked, and herringbone configurations. Films of 0.5% and 10% pentacene in *p*-terphenyl are studied, representative of the isolated molecule and partially aggregated systems respectively.[32] To account for the energetic and kinetic differences found experimentally, we perform density functional theory (DFT) calculations, providing the magnitude of the electronic coupling for the various configurations as well as the distribution of molecular orbitals over the coupled chromophore pairs. How orientation affects the thermodynamics of chromophores in the triplet state is a more fundamental question with implications not only in SF research but more generally pertaining to the understanding of excited state chromophore-chromophore interactions.

RESULTS & DISCUSSION

To investigate the excited state dynamics as a function of dimer configuration in solid-state systems, the temperature dependence of the time-resolved (tr) EPR spectra of thin films of pentacene in *p*-terphenyl were considered. Although the singlet fission mechanism itself is temperature independent,[33] the subsequent dissociation into free triplets and recombination to the ground state may be thermally activated depending on the dimer geometry. It is therefore important to understand how the

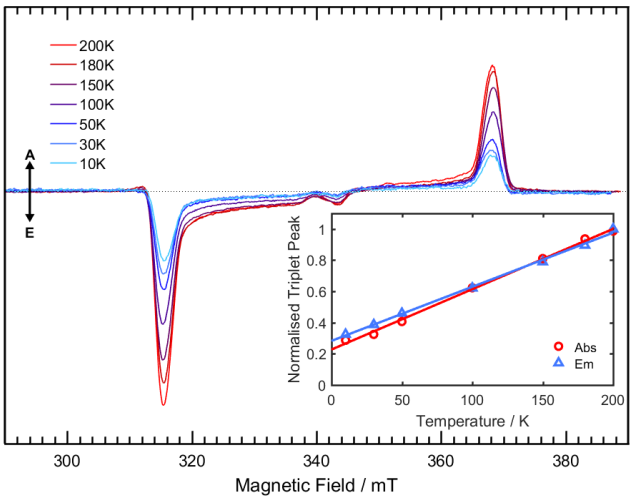

Figure 1. The tr-EPR spectra of the 1µm thick films of 0.5% pentacene in *p*-terphenyl, integrated over a 500-900 ns time window after the laser pulse. The data are taken as a function of temperature, with the long axis of the molecule aligned with the magnetic field. The maximum intensity for the emission (blue) and absorption (red) peaks are shown in the inset. A = enhanced absorption, E = emission.

molecular microstructure can affect the generation of polarons, impacting efficiency for potential photovoltaic applications. A thin film of 0.5% pentacene in *p*-terphenyl, a system of isolated molecules representative of the monomer photophysics, was first considered to determine the contribution of ISC triplets as a function of temperature. Intersystem crossing in pentacene is known to be temperature dependent as it is a vibronic assisted mechanism.[34,35] The tr-EPR spectra spanning temperatures from 200 K down to 10 K are reported in Figure 1, for the long axis of the pentacene molecule parallel to the magnetic field, with the maximum peak intensity plotted as a function of temperature in the inset. As temperature decreases, the pentacene triplet intensity decreases linearly, with the yield dropping to a third of its 200 K value by 10 K.

The temperature dependence of the tr-EPR spectra of the 10% pentacene film, representative of a partially aggregated system,[10,32] is shown in Figure 2, measured in the same conditions as the 0.5% film. The spectra are the superposition of three components: isolated triplets from ISC, parallel dimers and herringbone dimers contributing both triplet and quintet species, as reported previously.[10] The triplet to quintet (T/Q) peak ratio for each dimer configuration is reported in the inset as a function of temperature. The expectation would be a consistent ratio throughout all measurements due to the temperature independent nature of SF and this is indeed observed for the herringbone dimer (blue dots, Figure 2 inset). The intensity of herringbone quintets decreases proportionally to that of its triplets. Conversely, the T/Q ratio of the parallel dimer geometry decreases with decreasing temperature until 50 K, reaching approximately a quarter of its initial intensity before settling on a constant ratio. Comparing this with the dilute sample, it can be inferred that the additional triplet contribution at higher temperatures corresponds to the ISC monomer triplet, which eventually falls below the threshold of the temperature independent SF triplets. The decrease in T/Q ratio corresponds to the decrease in triplet intensity of the ISC triplet, as measured in

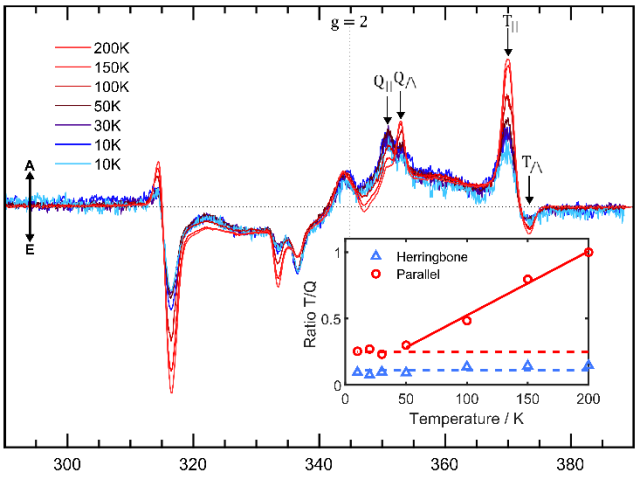

Figure 2. Temperature dependence of the photoexcited tr-EPR spectra of 10% pentacene in p-terphenyl with the long axis of the molecule parallel to the magnetic field. Inset shows the peak intensity ratios of the triplet and quintet peaks for herringbone and parallel dimer configurations as a function of temperature. A = enhanced absorption, E = emission.

the 0.5% pentacene sample. Furthermore, the increase in absolute intensity of the parallel quintet in the EPR spectra suggests that as temperature decreases and ISC is inhibited, SF then dominates with more quintets formed than at room temperature.

The Arrhenius equation relates the dependence of reaction rates on temperature as:

$$k = A \exp\left(-\frac{E_a}{RT}\right)$$

where A is a prefactor, E_a is the activation energy, R is the gas constant and T is temperature.

The decay rates of the ISC triplets back to the ground state for the 0.5% pentacene sample were calculated at each temperature and an Arrhenius plot reported in the supporting information. At ~190 K, *p*-terphenyl undergoes a phase change from a monoclinic to triclinic structure, allowing pentacene to substitute into four inequivalent sites instead of just two.[36,37] Most noticeably, the pentacene reordering results in a 20% decrease of the decay rate when lowering the temperature through the structural phase transition (See supporting Information Figure XXX). This has not been reported in the literature previously, as it is the first time a temperature dependent EPR study has been carried out through the phase change temperature of *p*-terphenyl. However, this could be significant in predicting optimal crystal structures for SF materials. The remaining data then follow the exponential increase in lifetime with decreasing temperature.

The temperature-dependent kinetics were then calculated for the 10% pentacene sample solving the ordinary differential rate equations for pentacene in *p*-terphenyl system [13,38] modified here to include both dimer configurations simultaneously:

$$\dot{Q}_{/\backslash} = k_{TQ_{/\backslash}} TT_{/\backslash} - (k_{diss_{/\backslash}} + k_{Qrec_{/\backslash}}) Q_{/\backslash} + \text{ratio}Q_{0/\backslash} * k_{irf} * S_1$$

$$\dot{TT}_{/\backslash} = -k_{TQ_{/\backslash}} TT_{/\backslash} + k_{diss_{/\backslash}} Q_{/\backslash} - k_{diff_{/\backslash}} TT_{/\backslash} - k_{TTrec_{/\backslash}} TT_{/\backslash}$$

$$\dot{Q}_{\|} = k_{TQ_{\|}} TT_{\|} - (k_{diss_{\|}} + k_{Qrec_{\|}}) Q_{\|} + \text{ratio}Q_{0\|} * k_{irf} * S_1$$

$$\dot{TT}_{\|} = -k_{TQ_{\|}} TT_{\|} + k_{diss_{\|}} Q_{\|} - k_{diff_{\|}} TT_{\|} - k_{TTrec_{\|}} TT_{\|}$$

$$\dot{T} = k_{diff_{\|}} TT_{\|} + k_{diff_{/\backslash}} TT_{/\backslash} - k_{Trec} T + \text{ratio}T_0 * k_{irf} * S_1$$

$$\dot{S}_0 = k_{Trec} T + k_{TTrec_{\|}} TT_{\|} + k_{Qrec_{\|}} Q_{\|} + k_{Qrec_{/\backslash}} Q_{/\backslash} + k_{TTrec_{/\backslash}} TT_{/\backslash}$$

$$\dot{S}_1 = -k_{irf} * S_1$$

where $\dot{Q}$ and $\dot{TT}$ are the quintet and dissociated triplets for the parallel, ||, and herringbone, /\, cases; $\dot{T}, \dot{S}_0$ and $\dot{S}_1$ are the monomer triplet, ground state and excited singlet state respectively. The model sets the starting population entirely in S_1, with a fitted triplet/quintet ratio parameter.

The kinetic parameters are the rate of dissociation, $k_{diss} = {}^5(TT) \rightarrow T + T$; the rate of back-transfer from triplets to quintet, $k_{TQ} = T + T \rightarrow {}^5(TT)$, the triplets decay, $k_{Trec} = T \rightarrow S_0$, and $k_{TTrec} = T + T \rightarrow S_0 + S_0$; and the quintet recombination to ground state, $k_{Qrec} = {}^5(TT) \rightarrow S_0 S_0$, with the corresponding configuration subscript where relevant. The fitted data is shown with a schematic of the kinetic model in Figure 3. As the spectral features corresponding to the parallel dimer triplet contribution consist of overlapping SF generated triplets and monomer triplets generated by ISC, the kinetic model includes both pathways and treats these independently. The triplet populations due to SF and ISC mechanisms are summed to generate a full kinetic spectrum. As the ISC contribution is temperature dependent, the proportion of ISC triplet is fitted at each temperature and returns a constant ratio at 50 K and below. Given that the proposed model considers all possible dynamic processes at once, even including the coupling between parallel and herringbone configurations, it requires a total of XXX parameters. To constrain the large number of parameters, an activation energy is included and limited to 5 meV.

Applying this model, it was found that simplifications of the rate equations were possible. Firstly, the activation energy was negligible in all rates except the quintet recombination to the ground state, confirming the long-standing knowledge that SF is a temperature independent mechanism. Only the quintet recombination to the ground state is thermally activated. Diffusion also proved to be a superfluous term. Previous structural work demonstrated that pentacene aggregates could not be larger than the XRD instrument resolution, namely 5 nm.[10,31] The lack of evidence for any diffusion suggests the films are homogenously blend to the molecular level, and no clusters are present even in the 10 % pentacene films. The rates of back-transfer from triplets to quintets were also found to be negligible irrespective of the dimer configuration. This is unsurprising considering the downhill energy landscape of singlet fission in pentacene. Dissociation is faster in the parallel dimer, as previously reported,[10] but this study proves the recombination to the ground state is also faster by an order of magnitude.

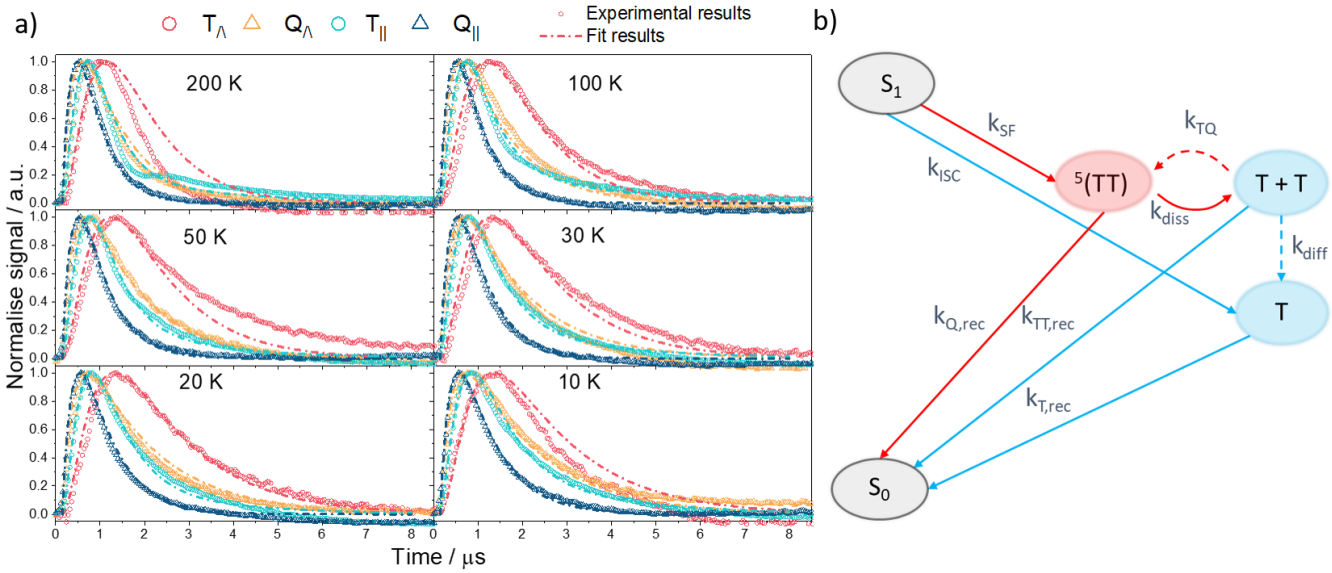

Figure 3. a) Photoexcited tr-EPR spectra of 10% pentacene in p-terphenyl measured with the molecule's long axis parallel to the magnetic field (open circles) and corresponding fits from the kinetic model (dashed lines). The 4 signal decays are from the herringbone triplets (red) and quintets (yellow) and parallel triplets (green) and quintets (blue). The different panels show the decay at different temperatures from 200 K to 10 K. b) Diagram illustrating the kinetic rates described by the differential equations given in the main text. The black, red and blue bubbles are the singlet quintet and triplet states respectively. The dotted lines represent the rates that are deemed negligible in this system

To understand the differing dynamics of the two dimer configurations, a number of DFT calculations were performed. The crystal structure of pentacene was used to optimise the dimers, though there may be slight variations in the herringbone angle of the dimers from dilution in the *p*-terphenyl matrix. As the crystal structure of the blends has yet to be determined, using the optimised pentacene structure provides a more appropriate comparison to the SF mechanism of pure pentacene systems. Therefore, from the pentacene crystal structure four inequivalent pairs of molecules were identified. These are the herringbone pair (HB), the slip-stacked parallel pair along the *a* cell axis (SS), the cofacial parallel along *b* cell axis (CP) and the head-to-tail parallel along *c* cell axis (HT), reported in SI (Figure 5), with the shortest distances between carbon atoms labelled. In the same figure we included the calculated hole and electron transfer integrals for all the three parallel dimers and the herringbone dimer. The electron and hole transfer integrals were calculated with a hybrid DFT molecular pair calculation with a (B3LYP/6.31g(d,p)) functional using the counterpoise method.[38]

EPR spectroscopy does not differentiate between the different parallel configurations as pairs are defined by the intermolecular angle, which is the same for all parallel configurations, however in DFT each pair is considered separately. Only molecules with nearest neighbour separations up to 4 Å have sufficiently strong intermolecular interactions from the π-π stacking to undergo transitions to CT states.[39–41] The CP dimer can therefore be excluded as participating in SF as the intermolecular separation is too large resulting in couplings only on the order of μeV. Similarly, the transfer integrals of the HT configuration are orders of magnitude weaker than for the HB and SS configurations, therefore only the latter are compared in this work. These calculations indicate that the parallel pair observed experimentally is most likely a SS dimer. Thus, in the following investigations we focus only on HB and SS dimers.

The orbitals calculated for the HB and SS geometries are shown in Figure 4. It was determined that in the herringbone geometry the orbitals are localised on one or the other molecule, whereas in the parallel geometries these are delocalised over both. It suggests that excitons in HB can have either charge-transfer character (charge in the exciton is separated) and in SS exciton would be delocalized over two units.

TD-DFT calculations of excited states and charge distribution confirmed those predictions. Energies and oscillator strengths of excited states for pentacene monomer and two dimers: HB and SS are presented in Table 2, charge distributions for the excited states are presented in SI (Table S5 and S6). The calculated energies are in relatively good agreement to those obtained experimentally.[10] The lowest triplet energies are close for both dimers and the same as for monomer, even though they are lower than experimental values. The differences between calculated and experimental energies are expected due to limitations in TD-DFT to accurately predict energies for large molecules.[42] The calculated electronic structure in HB dimer reveals CT character states (triplet and singlet) at relatively low energy, which could impact the performance. The symmetry of SS dimer enhances the delocalization of excited states, specifically for strongly absorbing singlet. The optoelectronic processes in HB dimer are therefore more probable to be CT mediated than those occurring in SS dimer.

Next, we considered interactions between excited states taking part in the singlet fission. SF processes involve doubly excited states, however calculations of those states and interaction between them are computationally expensive and would be a subject for a further study. [43] Therefore, here we study couplings between singly excited states, specifically low energy triplets, and connect them to doubly excited states for both dimer structures. Spin-orbit couplings between triplet and singlet ground state and transition dipole moments between excited states for pentacene monomer, HB and SS dimers were calculated using PySOC code implemented to Gaussian output.[44]

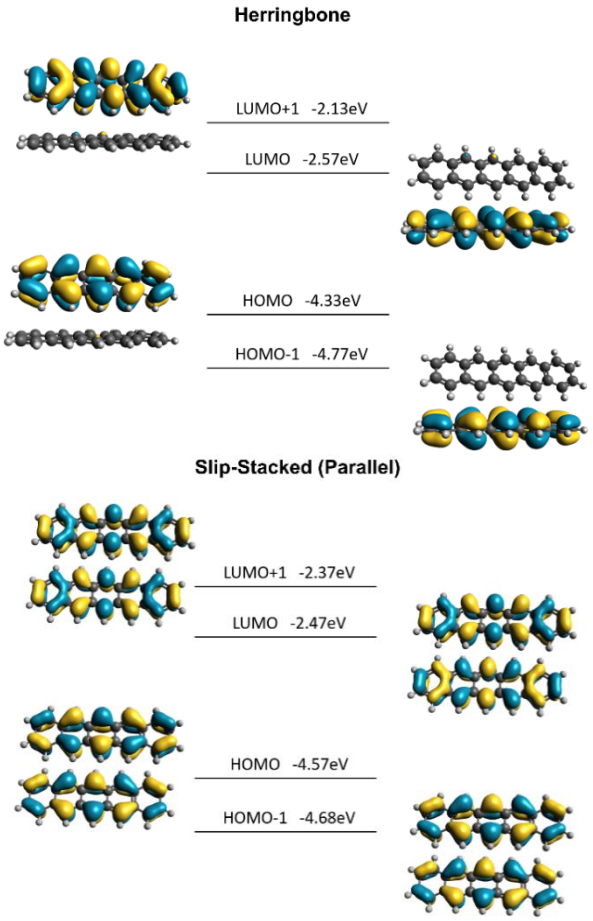

Figure 4. Calculated molecular orbitals for the pentacene monomer and the three dimer configurations that participate in SF: herringbone, slip-stacked and head-to-tail parallel.

The quintet dissociation process is often connected to spin coupling between triplets, and the electronic coupling is neglected. Here we study the correlation between electronic coupling and dissociation rate for two structures.

First, we look at the transition dipole moment (tdm) between two low energy triplets T_1 and T_2 in both dimers. We propose that transition dipole moment can be understood as an electronic coupling between states. The discussion based on the orbital transitions is included in SI. In Table 1 we present the calculated transition dipole moment between T_1 and T_2 for both dimers. There is a significant difference in tdm, and thus electronic coupling, between HB and SS structures. The magnitude of tdm between T_1 and T_2 is equal to 9.04 Debye and 0.02 Debye in HB and SS dimer respectively. Since the quintet state observed in SF process is a coupled triplet pair (T_1T_2), we propose that strong coupling between those triplets in HB dimer results in slower quintet dissociation than in SS dimer. It supports the idea that electronic coupling plays a role in dissociation process. However, considering that coupling is over 2 orders of magnitude higher and the dissociation rate only three times lower, there are other important interaction.

The recombination rate of correlated triplets also differs for two dimer structures and is around two times higher in SS than in HB dimer. This does not correspond with the calculated spin-

	HERRINGBONE	SLIP-STACKED
Dissociation rate at 200K (kinetic model)	0.6 μs^{-1}	1.58 μs^{-1}
Transition dipole moment $\langle T_1\|r\|T_2\rangle$	9.04 Debye	0.02 Debye

Table 1: Comparison between herringbone and slip-stacked dimer of dissociation rate at 200K obtained from the kinetic model and calculated transition dipole moment between triplets T_1 and T_2.

	Energy (eV)	Oscillator Strength	Character	$\langle S_0\|SOC\|T_n\rangle$
MONOMER				
T_1	0.60	0	-	0.000
T_2	1.89	0	-	0.696
S_1	1.91	0.0412	-	-
HERRINGBONE DIMER				
T_1	0.56	0	F	0.100
T_2	0.59	0	F	0.379
S_1	1.31	0.0071	CT	-
T_3	1.32	0	CT	0.337
T_4	1.87	0	F	1.059
T_5	1.89	0	F	0.527
S_2	1.91	0.0492	F	-
S_3	1.93	0.0258	F	-
SLIP-STACKED DIMER				
T_1	0.58	0	Delocalized	0.000
T_2	0.59	0		0.221
S_1	1.75	0.0527		-
T_3	1.79	0		0.302
S_2	1.79	0		-
T_4	1.80	0		0.000
T_5	1.88	0		1.086
T_6	1.89	0		0.000
S_3	1.95	0		-
S_4	1.97	0.0575		0.000

Table 2: Excited states calculated using TD-DFT for the pentacene monomer, herringbone dimer and parallel dimer. Character of each state was determined based on participating orbital transitions and confirmed by calculated charge distribution (presented in SI). In the last column spin-orbit coupling for the triplet to ground state interaction.

orbit couplings of T_1 and T_2 to ground state, as the sum of those is two times higher for HB than for SS. The nature of correlated triplet pair is not yet well understood. Here, we propose that the recombination dynamics of correlated triplet pair depends not only on the spin-orbit coupling to the S_0 ground state, but also on the interaction between these triplets. The correlated triplet pair is still considered to be (T_1+T_2) for dimer, rather than two T_1 for pentacene monomer. The recombination rate

for correlated triplets would be then interplay between the coupling to the ground and interaction between the triplets.

CONCLUSION

The work presented here details the effects of molecular orientation on the kinetics of the SF mechanism, to identify the optimal microstructure for efficient devices. This is of particular relevance as hybrid devices are being successfully engineered but still require significant optimisation,[6] which we postulate can be achieved through control of intermolecular geometries.

The systematic study of triplet and quintet species in dilute pentacene films, achieved using EPR spectroscopy at cryogenic temperatures, has enabled the ISC and SF triplets contributions to be distinguished and quantified. This demonstrates how a slight change in the microstructure, in this case from a monoclinic to a triclinic lattice, impacts the kinetics and could therefore be used to predict optimal crystal structures for SF. Exploiting the unique ability of EPR to distinguish between molecular configurations, the kinetic parameters for both dimer geometries were modelled simultaneously. Most processes required no thermal activation and diffusion was not required in the model. This is indicative of a homogenously blend down to the molecular scale with the lack of diffusion taken as an evidence of the effective dilution. Dissociation was found to be more efficient in parallel dimers, as previously reported, and this was confirmed using DFT calculations. It was found that the electronic coupling was weaker in the parallel configurations with orbitals delocalised over both molecules. Conversely, the herringbone dimer has orbitals localised on one molecule or other, resulting in excited states with charge transfer character, and high electronic coupling between triplets, which leads to inefficient dissociation. Our results demonstrate the important role of electronic coupling in the dynamics of singlet fission materials and its correlation to molecular configuration. Applying these findings to the design of efficient SF layers could enhance the efficiency of hybrid solar cells at the forefront of OPV development.

ASSOCIATED CONTENT

Experimental details; isolated molecule information and data; complete DFT results and molecular orbital diagrams.
This material is available free of charge via the Internet at http://pubs.acs.org.

AUTHOR INFORMATION

Corresponding Authors

* Professor Sandrine Heutz (s.heutz@imperial.ac.uk) and Dr Enrico Salvadori (enrico.salvadori@unito.it).

Present Addresses

†National High Magnetic Field Laboratory, 1800 E Paul Dirac Dr, Tallahassee, FL 32310.

Author Contributions

All authors have given approval to the final version of the manuscript.

Funding Sources

Any funds used to support the research of the manuscript should be placed here (per journal style).

Notes

Any additional relevant notes should be placed here.

ACKNOWLEDGMENT

D.L.P. acknowledges a studentship from the UK Engineering and Physical Sciences Research Council (EPSRC) Centre for Doctoral Training for the Advanced Characterisation of Materials (EP/L015277/1).

ABBREVIATIONS

LH2, LH light harvesting 2.

REFERENCES

(1) Zhang, J. P.; Inaba, T.; Watanabe, Y.; Koyama, Y. Partition of Carotenoid-to-Bacteriochlorophyll Singlet-Energy Transfer through Two Channels in the LH2 Complex from Rhodobacter Sphaeroides G1C. *Chem. Phys. Lett.* **2001**, *340*, 484. https://doi.org/10.1016/S0009-2614(01)00451-1.

(2) Polli, D.; Cerullo, G.; Lanzani, G.; De Silvestri, S.; Hashimoto, H.; Cogdell, R. J. Carotenoid-Bacteriochlorophyll Energy Transfer in LH2 Complexes Studied with 10-Fs Time Resolution. *Biophys. J.* **2006**, *90*, 2486. https://doi.org/10.1529/biophysj.105.069286.

(3) Tabernig, S. W.; Daiber, B.; Wang, T.; Ehrler, B. Enhancing Silicon Solar Cells with Singlet Fission: The Case for Förster Resonant Energy Transfer Using a Quantum Dot Intermediate. *J. Photonics Energy* **2018**, *8* (02), 1. https://doi.org/10.1117/1.JPE.8.022008.

(4) MacQueen, R.; Liebhaber, M.; Niederhausen, J.; Mews, M.; Gersmann, C.; Jäckle, S.; Jäger, K.; Tayebjee, M. J. Y.; Schmidt, T. W.; Rech, B.; et al. Crystalline Silicon Solar Cells with Tetracene Interlayers: The Path to Silicon-Singlet Fission Heterojunction Devices. *Mater. Horizons* **2018**, *5*, 1065. https://doi.org/10.1039/C8MH00853A.

(5) Davis, N. J. L. K.; Allardice, J. R.; Xiao, J.; Petty, A. J.; Greenham, N. C.; Anthony, J. E.; Rao, A. Singlet Fission and Triplet Transfer to PbS Quantum Dots in TIPS- Tetracene Carboxylic Acid Ligands. *J. Phys. Chem. Lett.* **2018**, *9*, 1454–1460. https://doi.org/10.1021/acs.jpclett.8b00099.

(6) Einzinger, M.; Wu, T.; Kompalla, J. F.; Smith, H. L.; Perkinson, C. F.; Nienhaus, L.; Wieghold, S.; Congreve, D. N.; Kahn, A.; Bawendi, M. G.; et al. Sensitization of Silicon by Singlet Exciton Fission in Tetracene. *Nature* **2019**, *571* (7763), 90–94. https://doi.org/10.1038/s41586-019-1339-4.

(7) Musser, A. J.; Clark, J. Triplet-Pair States in Organic Semiconductors. *Annu. Rev. Phys. Chem.* **2019**, *70*, 323.

(8) Tayebjee, M. J. Y.; Sanders, S. N.; Kumarasamy, E.; Campos, L. M.; Sfeir, M. Y.; McCamey, D. R. Quintet Multiexciton Dynamics in Singlet Fission. *Nat. Phys.* **2017**, *13* (2), 182–188. https://doi.org/10.1038/nphys3909.

(9) Weiss, L. R.; Bayliss, S. L.; Kraffert, F.; Thorley, K. J.; Anthony, J. E.; Bittl, R.; Friend, R. H.; Rao, A.; Greenham, N. C.; Behrends, J. Strongly Exchange-Coupled Triplet Pairs in an Organic Semiconductor. *Nat. Phys.* **2017**, *13* (October), 176–181. https://doi.org/10.1038/nphys3908.

(10) Lubert-Perquel, D.; Salvadori, E.; Dyson, M.; Stavrinou, P. N.; Montis, R.; Nagashima, H.; Kobori, Y.; Heutz, S.; Kay, C. W. M. Identifying Triplet Pathways in Dilute Pentacene Films. *Nat. Commun.* **2018**, *9*, 4222. https://doi.org/10.1038/s41467-018-06330-x.

(11) Fallon, K. J.; Budden, P.; Salvadori, E.; Ganose, A. M.; Savory, C. N.; Eyre, L.; Dowland, S.; Ai, Q.; Goodlett, S.; Risko, C.; et al. Exploiting Excited-State Aromaticity to Design Highly Stable Singlet Fission Materials. *J. Am. Chem. Soc.* **2019**, *141* (35), 13867–13876. https://doi.org/10.1021/jacs.9b06346.

(12) Smith, M. B.; Michl, J. Recent Advances in Singlet Fission. *Annu.*

Rev. Phys. Chem. **2013**, *64*, 361–386. https://doi.org/10.1146/annurev-physchem-040412-110130.

(13) Dover, C. B.; Gallaher, J. K.; Frazer, L.; Tapping, P. C.; Petty, A. J.; Crossley, M. J.; Anthony, J. E.; Kee, T. W.; Schmidt, T. W. Endothermic Singlet Fission Is Hindered by Excimer Formation. *Nat. Chem.* **2018**, *10* (3), 305–310. https://doi.org/10.1038/nchem.2926.

(14) Stern, H. L.; Musser, A. J.; Gelinas, S.; Parkinson, P.; Herz, L. M.; Bruzek, M. J.; Anthony, J.; Friend, R. H.; Walker, B. J. Identification of a Triplet Pair Intermediate in Singlet Exciton Fission in Solution. *Proc. Natl. Acad. Sci.* **2015**, *112* (25), 7656–7661. https://doi.org/10.1073/pnas.1503471112.

(15) Merrifield, R. E. Magnetic Effects on Triplet Exciton Interactions. *Pure Appl. Chem.* **1971**, *27* (3), 481–498. https://doi.org/10.1351/pac197127030481.

(16) Yago, T.; Ishikawa, K.; Katoh, R.; Wakasa, M. Magnetic Field Effects on Triplet Pair Generated by Singlet Fission in an Organic Crystal: Application of Radical Pair Model to Triplet Pair. *J. Phys. Chem. C* **2016**, *120* (49), 27858–27870. https://doi.org/10.1021/acs.jpcc.6b09570.

(17) Yost, S. R.; Lee, J.; Wilson, M. W. B.; Wu, T.; McMahon, D. P.; Parkhurst, R. R.; Thompson, N. J.; Congreve, D. N.; Rao, A.; Johnson, K.; et al. A Transferable Model for Singlet-Fission Kinetics. *Nat. Chem.* **2014**, *6* (6), 492–497. https://doi.org/10.1038/nchem.1945.

(18) Basel, B. S.; Zirzlmeier, J.; Hetzer, C.; Phelan, B. T.; Krzyaniak, M. D.; Reddy, S. R.; Coto, P. B.; Horwitz, N. E.; Young, R. M.; White, F. J.; et al. Unified Model for Singlet Fission within a Non-Conjugated Covalent Pentacene Dimer. *Nat. Commun.* **2017**, *8* (May), 15171. https://doi.org/10.1038/ncomms15171.

(19) Tayebjee, M. J. Y.; Sanders, S. N.; Kumarasamy, E.; Campos, L. M.; Sfeir, M. Y.; McCamey, D. R. Quintet Multiexciton Dynamics in Singlet Fission. *Nat. Phys.* **2017**, *13* (2), 182–188. https://doi.org/10.1038/nphys3909.

(20) Zimmerman, P. M.; Bell, F.; Casanova, D.; Head-Gordon, M. Mechanism for Singlet Fission in Pentacene and Tetracene : From Single Exciton to Two Triplets. *J. Am. Chem. Soc.* **2011**, *133*, 19944–19952. https://doi.org/10.1021/ja208431r.

(21) Tamura, H.; Huix-rotllant, M.; Burghardt, I.; Olivier, Y.; Beljonne, D. First-Principles Quantum Dynamics of Singlet Fission : Coherent versus Thermally Activated Mechanisms Governed by Molecular π Stacking. *Phys. Rev. Lett.* **2015**, *115*, 107401. https://doi.org/10.1103/PhysRevLett.115.107401.

(22) Monahan, N. R.; Sun, D.; Tamura, H.; Williams, K. W.; Xu, B.; Zhong, Y.; Kumar, B.; Nuckolls, C.; Harutyunyan, A. R.; Chen, G.; et al. Dynamics of the Triplet-Pair State Reveals the Likely Coexistence of Coherent and Incoherent Singlet Fission in Crystalline Hexacene. *Nat. Chem.* **2016**, *9* (4), 341–346. https://doi.org/10.1038/nchem.2665.

(23) Sutton, C.; Tummala, N. R.; Beljonne, D.; Bredas, J. L. Singlet Fission in Rubrene Derivatives : Impact of Molecular Packing. *Chem. Mater.* **2017**, *29*, 2777–2787. https://doi.org/10.1021/acs.chemmater.6b04633.

(24) Okada, K.; Tonami, T.; Nagami, T.; Nakano, M. Breakdown of the Perturbative Approach to Molecular Packing Dependence of Singlet Fission Rates in Pentacene Dimer Models : A Systematic Comparison with the Quantum Master Equation Approach. *J. Phys. Chem. C* **2019**, *123*, 15403–15411. https://doi.org/10.1021/acs.jpcc.9b01713.

(25) Shushin, A. I. Kinetics of Singlet Fission in Organic Semiconductors: Specific Features of T-Exciton Migration Effects. *J. Chem. Phys.* **2019**, *151* (3). https://doi.org/10.1063/1.5099667.

(26) Lee, T. S.; Lin, Y. L.; Kim, H.; Rand, B. P.; Scholes, G. D. Two Temperature Regimes of Triplet Transfer in the Dissociation of the Correlated Triplet Pair after Singlet Fission. *Can. J. Chem.* **2019**, *97* (6), 465–473. https://doi.org/10.1139/cjc-2018-0421.

(27) Zaykov, A.; Felkel, P.; Buchanan, E. A.; Jovanovic, M.; Havenith, R. W. A.; Kathir, R. K.; Broer, R.; Havlas, Z.; Michl, J. Singlet Fission Rate: Optimized Packing of a Molecular Pair. Ethylene as a Model. *J. Am. Chem. Soc.* **2019**. https://doi.org/10.1021/jacs.9b08173.

(28) Margulies, E. A.; Shoer, L. E.; Eaton, S. W.; Wasielewski, M. R. Excimer Formation in Cofacial and Slip-Stacked Perylene-3,4:9,10-Bis(Dicarboximide) Dimers on a Redox-Inactive Triptycene Scaffold. *Phys. Chem. Chem. Phys.* **2014**, *16*, 23735–23742. https://doi.org/10.1039/c4cp03107e.

(29) Chen, M.; Bae, Y. J.; Mauck, C. M.; Mandal, A.; Young, R. M.; Wasielewski, M. R. Singlet Fission in Covalent Terrylenediimide Dimers: Probing the Nature of the Multiexciton State Using Femtosecond Mid-Infrared Spectroscopy. *J. Am. Chem. Soc.* **2018**, *140*, 9184–9192. https://doi.org/10.1021/jacs.8b04830.

(30) Mandal, A.; Chen, M.; Foszcz, E. D.; Schultz, J. D.; Kearns, N. M.; Young, R. M.; Zanni, M. T.; Wasielewski, M. R. Two-Dimensional Electronic Spectroscopy Reveals Excitation Energy-Dependent State Mixing during Singlet Fission in a Terrylenediimide Dimer. *J. Am. Chem. Soc.* **2018**, *140*, 17907–17914. https://doi.org/10.1021/jacs.8b08627.

(31) Wang, X.; Liu, X.; Tom, R.; Cook, C.; Schatschneider, B. Phenylated Acene Derivatives as Candidates for Intermolecular Singlet Fission. *J. Phys. Chem. C* **2019**, *123*, 5890–5899. https://doi.org/10.1021/acs.jpcc.8b12549.

(32) Lubert-Perquel, D.; Kim, D. K.; Robaschik, P.; Kay, C. W. M.; Heutz, S. Growth, Morphology and Structure of Mixed Pentacene Films. *J. Mater. Chem. C* **2019**, *7*, 289–196. https://doi.org/10.1039/c8tc05525d.

(33) Stern, H. L.; Cheminal, A.; Yost, S. R.; Broch, K.; Bayliss, S. L.; Chen, K.; Tabachnyk, M.; Thorley, K.; Greenham, N.; Hodgkiss, J. M.; et al. Vibronically Coherent Ultrafast Triplet-Pair Formation and Subsequent Thermally Activated Dissociation Control Efficient Endothermic Singlet Fission. *Nat. Chem.* **2017**, *9* (12), 1205–1212. https://doi.org/10.1038/nchem.2856.

(34) Patterson, F. G.; Lee, H. W. H.; Wilson, W. L.; Fayer, M. D. Intersystem Crossing from Singlet States of Molecular Dimers and Monomers in Mixed Molecular Crystals: Picosecond Stimulated Photon Echo Experiments. *Chem. Phys.* **1984**, *84* (1), 51–60. https://doi.org/10.1016/0301-0104(84)80005-1.

(35) El-Sayed, M. A.; Olmsted III, J. Intersystem Crossing Relative Rates from Pulsed-Excitation Phosopherence Microwave Double-Resonance. *Chem. Phys. Lett.* **1971**, *11* (5), 568.

(36) da Costa, A. A. M.; Amado, A. M.; Becucci, M.; Kryschi, C. Order-Disorder Phase Transition in p-Terphenyl and p-Terphenyl:Tetracene Doped Crystals as Studied by Raman Spectrsocopy. *J. Mol. Struct.* **1997**, *416*, 69–73.

(37) Lang, J.; Sloop, D. J.; Lin, T.-S. Dynamics of P-Terphenyl Crystals at the Phase Transition Temperature: A Zero-Field EPR Study of the Photoexcited Triplet State of Pentacene in p-Terphenyl Crystals. *J. Phys. Chem. A* **2007**, *111* (22), 4731–4736. https://doi.org/10.1021/jp070251v.

(38) Sakai, H.; Inaya, R.; Nagashima, H.; Nakamura, S.; Kobori, Y.; Tkachenko, N. V.; Hasobe, T. Multiexciton Dynamics Depending on Intramolecular Orientations in Pentacene Dimers : Recombination and Dissociation of Correlated Triplet Pairs. *J. Phys. Chem. Lett.* **2018**, *9*, 3354. https://doi.org/10.1021/acs.jpclett.8b01184.

(39) Hestand, N. J.; Spano, F. C. Molecular Aggregate Photophysics beyond the Kasha Model: Novel Design Principles for Organic Materials. *Acc. Chem. Res.* **2017**, *50* (2), 341–350. https://doi.org/10.1021/acs.accounts.6b00576.

(40) Gisslén, L.; Scholz, R. Crystallochromy of Perylene Pigments: Interference between Frenkel Excitons and Charge-Transfer States. *Phys. Rev. B - Condens. Matter Mater. Phys.* **2009**, *80* (11), 1–23. https://doi.org/10.1103/PhysRevB.80.115309.

(41) Hoffmann, M.; Soos, Z. G. Optical Absorption Spectra of the Holstein Molecular Crystal for Weak and Intermediate Electronic Coupling. *Phys. Rev. B - Condens. Matter Mater.*

Phys. **2002**, *66* (2), 243051–2430518. https://doi.org/10.1103/PhysRevB.66.024305.

For Table of Contents Only